Cellular Physiology and Biochemistry

Cell Physiol Biochem 2018;49:1184-1203
DOI: 10.1159/000493296
Published online: 6 September, 2018
Accepted: 28 August, 2018

Original Paper

S100A4 Knockout Sensitizes Anaplastic Thyroid Carcinoma Cells Harboring BRAF$^{V600E/Mt}$ to Vemurafenib

Xuelong Jiao[a] Hongmei Zhang[b] Xiangpeng Xu[b] Ying Yu[b] Honglai Zhang[b] Jinna Zhang[b] Liang Ning[a] Fengyun Hao[c] Xinfeng Liu[d] Min Niu[e] Chen-Tong Chen[f] Dong Chen[a] Kejun Zhang[b]

[a]Department of General Surgery, the Affiliated Hospital of Qingdao University, Qingdao, [b]Department of Thyroid Surgery, the Affiliated Hospital of Qingdao University, Qingdao, [c]Department of Pathology, the Affiliated Hospital of Qingdao University, Qingdao, [d]Department of Nuclear Medicine, the Affiliated Hospital of Qingdao University, Qingdao, [e]Department of Pharmacy, the Affiliated Hospital of Qingdao University, Qingdao, Shandong, China, [f]McGill Division of General Surgery, McGill University, Healthy Center, Montreal, Canada

Key Words
Anaplastic thyroid cancer • BRAF • S100A4 • Vemurafenib

Abstract
Background/Aims: Anaplastic thyroid cancer (ATC), with 25% BRAF^{V600E} mutation, is one of the most lethal human malignancies that currently has no effective therapy. Vemurafenib, a BRAFV600E inhibitor, has shown promise in clinical trials, including ATC patients, but is being hampered by the acquisition of drug resistance. Therefore, combination therapy that includes BRAF^{V600E} inhibition and avoids resistance is a clinical need. ***Methods:*** ATC cell lines 8505C $^{(BRAFV600E/mt)}$, SW1736 $^{(BRAFV600E/mt)}$, KAT18 $^{(BRAFV600E/wt)}$ and Cal-62$^{(BRAFV600E/wt)}$ cells were used in the study. The ability of S100A knockout or /and in combination with the BRAF inhibitor vemurafenib on growth, apoptosis, invasion and apoptosis in ATC cells *in vitro* was demonstrated by MTT and BrdUrd incorporation assay, Annexin-V-FITC staining analyzed by flow cytometry, Transwell migration and Matrigel invasion assay. S100A4,pERK1/2, pAKT and pROCK1/2 protein was detected by western blot assay; Small molecule inhibitors of Y27632, U0126, MK-2206 and constitutively active forms of pCDNA-Myc-pERK, pCMV6-HA-Akt, pCMV-RhoA were employed, and the mechanistic studies were performed. We assessed the efficiency of *in vivo* combination treatment with S100A4 knockout and Vemurafenib on tumors. ***Results:*** S100A4 knockout induced apoptosis and reduced proliferation by inactivation of pAKT and pERK signals, and inhibited invasion and migration by inactivation of pAKT and RhoA/ROCK1/2 signals in 8505C or Cal-62 cells *in vitro*, and vice versa in SW1736 and KAT18 cells. Vemurafenib did not affect apoptosis of both 8505C and SW1736 cells, but reduced proliferation via arresting cell cycle, and promoted cell migration and invasion *in vitro*. Combination treatment with S100A4 knockdown and vemurafenib reduced cell proliferation,

Kejun Zhang
and Dong Chen

Department of Thryoid Surgery, The Affiliated Hospital of Qingdao University
Qingdao, Shandong (China)
E-Mail thyroid_molecule@126.com; chendd820@126.com

migration and invasion *in vitro* compared to the S100A4 knockdown or Vemurafenib alone. Vemurafenib treatment resulted in a transient inhibition of pERK expression and gradually activation of pAKT expression, but quickly recovery from ERK1/2 activation inhibition by vemurafenib treatment in 4 h for SW1736 and 8505C cells. Combined treatment completely inhibited ERK1/2 and AKT activation during 48 h. In an *in vivo* mouse model of SW1736 and 8505C, vemurafenib treatment alone did not significantly inhibit tumor growth in both of the tumors, but inhibited tumor growth in combined groups. ***Conclusion:*** Our results show S100A4 knockout alone inhibits ATC cells (rich endogenous S100A4) survival and invasion, regardless of the $BRAF^{V600E}$ status, and potentiates the effect of vemurafenib on tumor regression *in vitro* and *in vivo*. In addition, S100A4 knockout potently inhibits the recovery from ERK1/2 activation inhibition and the AKT activation following vemurafenib treatment and reversed the vemurafenib resistance. This therapeutic combination may be of benefit in patients with ATC.

Introduction

Thyroid cancer are the most common malignancy of the endocrine system [1].Well-differentiated thyroid carcinomas account for > 90% of all thyroid cancers and include papillary (PTC) and follicular carcinomas (FTC), which typically have an excellent prognosis. Undifferentiated (anaplastic) thyroid carcinoma (ATCs) accounts for 2% to 5% of all thyroid cancers, but accounts for 14-39% of thyroid carcinoma deaths and the median survival of 6 months [2, 3]. However, there are few interventions that have improved survival. Therefore, alternative systemic treatment for ATC are urgently needed.

The Ras/Raf/MAPK kinase (MEK) /MAPK/ERK (MAPK) pathway, driven by the $BRAF^{V600E}$ mutation and other genetic alterations, plays a fundamental role in thyroid tumorigenesis [4]. The phosphatidylinositol 3-kinase (PI3K)/Akt pathway, driven by various genetic alterations similarly plays an important role in thyroid tumorigenesis [5]. In fact, most of the ATCs harbored genetic mutations that could potentially dually activate the MAPK and PI3K/Akt pathways [6]. $B\text{-}Raf^{V600E}$ oncoprotein is a potent transforming factor that causes human thyroid cancer cell progression *in vitro* and *in vivo* [7]. The mutant $B\text{-}Raf^{V600E}$ protein results from a transversion (T1799A) in exon 15 of the *B-Raf* gene, which causes a valine-for-glutamate substitution at residue 600 of the protein. This mutation induces a conformational change in the protein that constitutively activates the MAPK pathway (*i.e*. ERK1/2) [8]. Using RNA interference (siRNA) to knock down BRAF in human ATC cell lines, preclinical studies showed the importance of BRAF for intracellular MAPK signaling and proliferation, as tumor growth was significantly inhibited [9, 10]. These findings suggested that BRAF could be an effective target for thyroid cancer treatment.

Vemurafenib/PLX4032 is a selective small molecule inhibitor of B-RafV600E, showing a preferential inhibition of cell proliferation, migration, and invasion of BRAFV600E human ATC cell lines [10-13]. Furthermore, vemurafenib decreased tumor growth and aggressiveness in an animal model using human ATC cell lines [11, 13]. Recently, a 51-year-old man with BRAF-mutated ATC responded well to vemurafenib, and showed nearly complete clearing of metastatic disease after 38 days' treatment [14]. Another case of an 80-year-old female patient with a BRAFV600E mutation bearing ATC showed an excellent and sustained response to single agent, vemurafenib, which may be able not only to induce rapid tumor regression, but also to sustain it in select instances, and the response was sustained for 61 weeks [15]. In addition, responses in patients treated with the BRAF inhibitor vemurafenib have exhibited modest activity. Direct inhibition of aberrantly activated BRAF (i.e., vemurafenib treatment) has shown some effectiveness, but only in a subset of patients and with the eventual development of resistance in most cases. In response to Pvemurafenib, selective RAF inhibitors such as vemurafenib can lead to paradoxically increased ERK signaling, especially in settings where there is upstream pathway activation, such as with RAS mutations and low to moderate RAF inhibitor doses [16]. Therefore, an unmet need remains: to develop additional molecularly targeted agents for treatment of these patients.

S100A4 belongs to the S100 family of Ca^{2+}-binding proteins and highly expressed in various metastatic tumour cells, involved in the regulation of various important cellular functions such as cell proliferation [17, 18], invasion and migration [17, 19-21], and cell-cell communication [22]. In addition, S100A4 contributes to chemoresistance and inhibition of apoptosis in pancreatic cancer cells [23]. S100A4 overexpression was present in most advanced thyroid carcinomas and lymph node metastases, and was associated with poor prognosis [24], and therapeutic targeting of S100A4 may successfully reduce local invasion and metastasis in thyroid carcinoma [22]. Furthermore, extracellular S100A4 consistently activated ERK signaling in thyroid cancer cells and induced PTEN/PI3K/AKT signaling in breast cancer cells, resulting in cell growth and migration [21, 25]. Targeting the BRAF and/or MEK kinases also rely on reactivation of the RAS-RAF-MEK-ERK mitogen-activated protein kinase (MAPK) signal transduction pathway, on activation of the alternative, PI(3)K-AKT-mTOR, pathway (which is ERK independent) [26]. We therefore suggested that combination targeting S100A4 and BRAF enforces the anti-tumor effect in ATCs.

It has demonstrated that the majority of BRAF-mutant thyroid cancer cell lines have proven to be resistant to vemurafenib, including ATC patients, and the reason for this disparity remains unclear. Herein, we report a novel resistance mechanism to vemurafenib in $BRAF^{V600E/mt}$ ATC cells, which is mediated via S100A4 dependent PI3K/AKT and ERK1/2 pathway and recovery from ERK1/2 activation inhibition by vemurafenib treatment. We also show that combination treatment with S100A4 knockdown and vemurafenib leads to marked increases in therapeutic efficacy in 8505C $^{(BRAFV600E/mt)}$, SW1736 $^{(BRAFV600E/mt)}$ *in vitro* and xenograft models. Taken together, our results indicate that combination treatment with S100A4 knockdown and vemurafenib could re-sensitize $BRAF^{MT}$ ATCs to vemurafenib and be potential novel treatment strategies for $BRAF^{BRAFV600E/mt}$ ATC.

Materials and Methods

Ethics statement

The study was conducted in accordance with the ethical standards and the Declaration of Helsinki and according to the national and international guidelines and was approved by the affiliated hospital of Qingdao University, Qingdao, China.

Cell lines

8505c $BRAF^{V600E/mt}$ was obtained from the German Collection of Microorganisms and Cell Culture (DSMZ, Braunschweig, Germany). CAL62 $BRAF^{V600E/wt}$ was not obtained directly from the DSMZ repository, but analyzed for polymorphisms and confirmed versus published data [27]. SW1736 were purchased from CLS Cell Lines Service GmbH (Germany). The human metastatic ATC-derived cell line $KAT18^{V600E/wt}$ were obtained from K. Ain (University of Kentucky, Lexington, KY). CAL62, 8505C and SW1736 were maintained in RPMI1640 medium and sodium bicarbonate (2.0 g/L). KAT18 was maintained in (DMEM) with sodium pyruvate (1 mmol/L) and sodium bicarbonate (2.2 g/L). ATC cell lines were supplemented with 10% fetal bovine serum (FBS) and Penicillin (100 units/ml)/streptomycin (100 µg/ml) (Gibco, Grand Island, NY, USA). The cells were maintained in continuous monolayer cultures at 37°C and 5% CO_2 humidified incubator at 37°C, expanded up to 70-80% confluence and then employed for the experiments as described below. To avoid cross-contamination, cell lines were separately cultured in a sterile tissue culture hood, which was UV irradiated between each cell line, and a separate bottle of media was used for each cell line. *All* these cell lines matched their respective STR profiles shown in previously published studies [27, 28], and/or in the German Collection of Microorganisms and Cell Cultures (DSMZ) and European Collection for Cell Cultures (ECACC) databases at all loci tested in common [29].

Antibodies and reagents

The following antibodies were used: *S100A4 (ab41532)(*Cambridge, MA, USA*);* phospho-Akt (Ser473) clone D9E, from Cell Signaling Technology), Total-AKT (1:1000, Cell Signaling Technology); phospho-ERK 1/2((T202/Y204) (Cell Signaling Technology, Cat # 4377), Total-ERK1/2 (Santa Cruz, Dallas, TX, Cat # sc-

94) ; RhoA (sc-418) (Santa Cruz, CA), phosphorylated (P) P-ROCK2 (T249, #ab83514, Abcam, Cambridge, UK),unphosphorylated/general (G) G-ROCK2 (#610624) (both from BD Biosciences, Heidelberg, Germany); BRAF (sc-5284)(Santa Cruz Biotechnology); Ki67 (Santa Cruz sc-7846); Actin from Sigma-Aldrich; ROCK2 inhibitor Y27632 (Calbiochem, 688000); pan-MEK inhibitor U0126 (Promega); Pan-Akt inhibitors: MK-2206 (Selleck chemicals); BRAF V600E inhibitor (vemurafenib)(Chemie Tek, Indianapolis, IN). Vemurafenib was dissolved in dimetylsulfoxic (DMSO) (Fisher Scientific, Morristown, NJ). DMSO alone was used as vehicle control at the concentration of 0.3% (equivalent to the percentage of DMSO in vemurafenib, Y27632 and U0126 treated cells).

Plasmids

S100A4 human shRNA expression plasmids targeting S100A4-mRNA (pLKO.1- S100A4 shRNA) and the control pLKO.1-shGFP plasmid (empty vector, RHS4080) were purchased from Open Biosystems (ThermoFisher Scientific, Waltham, MA, USA).The targeting sequence for S100A4-mRNA was 5'-GCUCAACAAGUCAGAACUAAA-3', RHS3979-9620807. The pCMV6-XL5-S100A4 cDNA (abbreviated as pCMV-S100A4) expression plasmid and control plasmid pCMV6-XL5 (pCMV) were purchased from OriGene Technologies. pCMV6-HA-Akt expression vectors were constructed from OriGene Technologies. pCDNA-Myc-pERK for ATC expression were obtained from Addgene. They are used for ATC cell re-expressing AKT or ERK. To construct the RhoA expression vector, the full-length wild type cDNA of human RhoA gene was subcloned into the expression vector pCMV6-XL5 (OriGene Technologies), and resulting clones were sequenced for the confirmation of successful subcloning of WT-RhoA cDNA (pCMV-RhoA).

Generation of S100A4-shRNA or S100A4-cDNA or others model cells

ATC cells stably expressing S100A4-shRNA (short hairpin RNA) were generated using the Lipofectamine 2000 CD (Invitrogen) reagent and were selected with G418 selection (400 μg/mL). The targeting sequence for S100A4-mRNA was 5'-GCUCAACAAGUCAGAACUAAA-3', RHS3979-9620807. Transient knockdown of S100A4 was achieved using siGenome SMARTpool siRNA (Thermo Fisher Scientific Dharmacon, Waltham, MA, USA).

To conduct the *cells re*-expressing S100A4-cDNA, ATC cells were transfected with either control pCMV6-XL5 vector or pCMV-S100A4 plasmid. Transfections were performed with Lipofectin 2000™ according to the manufacturer's protocol, and confirmed by Western blotting.

For analysis of RhoA/ROCK1/2 or AKT or ERK pathway activation, the stable S100A4-shRNA transfected ATC cells were re-transfected with either control vector or pCMV-RhoA or pCMV6-HA-Akt or pCDNA-Myc-pERK expression plaismids using Lipofectin 2000™ according to the manufacturer's protocol and confirmed by Western blotting. All plaismids were utilized at a final concentration of 100 nM. Cells were transfected for 48 h before subsequent treatment or analysis.

Inhibitor treatments

Y27632, U0126,MK-2206 were prepared as 10 mM stock solutions in DMSO, following the manufacturer's instructions. For analysis of RhoA/ROCK1/2 or AKT or ERK pathway inhibition, the ATC cells were treated with 10μM doses of inhibitors (Y27632, U0126, MK-2206 or triple-drug together) for 6 h (after 6 hours' treatment, RhoA/ROCK1/2, Akt and ERK phosphorylation was completely inhibited) , then transfected with pCMV6-XL5 vector or pCMV-S100A4 plasmid for 48 h, respectively. For analysis the effect of S100A4 knockdown or/and vemurafenib on ATC cells, the ATC cells or S100A4 shRNA transfected ATC cells were treated with 2μM doses of vemurafenib for 72h.

Western blot assay

Cell lysis and protein sample preparation was carried out as previously described [30]. Western blotting analysis was performed using standard techniques as described previously [31], using the following antibodies: anti-S100A4, anti-BRAF, anti-pAKT (Ser473), anti-pERK1/2(T202/Y204), anti-RhoA (sc-418), anti-pROCK1/2, anti-k67, anti-AKT and anti-ERK1/2. The probe proteins were detected using an enhanced chemiluminescence system (Amersham Life Sciences) according to the manufacturer's instructions.

Cell cycle and apoptotic assay

Treated ATC cells (10^6 cells) in different groups was harvested, washed with ice cold PBS, and fixed with 70% ethanol at -20 °C for 1h, then stained with Annexin-V-FITC antibody and PI for 15 minutes and the samples were analyzed by flow cytometry within 1 hour according to the previous description [32].

Cell viability and proliferation assay

Cell viability was assessed by 3-[4, 5-dimethylthiazol-2-yl]-2, 5 diphenyl tetrazolium bromide (MTT) assays. Treated ATC cells (3×10^3 cells) in different groups were performed as described previously [33]. Cell proliferation was assessed by bromodeoxyuridine (BrdUrd) incorporation, cells were incubated with BrdUrd (Invitrogen) for 60 minutes, then the proliferation of cells was monitored by a cell proliferation ELISA BrdUrd (colorimetric) kit (Roche), according to the manufacturers protocol.

Transwell migration

Transwell migration assays were assayed as previously described [34]. Briefly, treated ATC cells (10^5 cells) in different groups were seeded onto transwell inserts (8 μm pore; Costar, Corning, NY) coated with 0.2% gelatin, respectively. 24 hs later, the cells that had invaded the Matrigel and moved to the other side of the membrane were fixed and stained as in the migration assays. We typically observed 100-150 cells/field for control conditions. Each experiment was repeated in triplicate and the results were averaged. Statistical analysis was done using the Student's *t*test.

Matrigel invasion assay

Invasion assay was performed in Corning Transwell inserts coated with Matrigel. Treated ATC cells (10^5 cells) in different groups were seeded at a density of 1×10^5 per insert and cultured overnight. After 16 h of serum starvation, the cells were trypsinized, re-suspended in the low serum media. After 24 hr, the chambers were washed with PBS twice and the cells on the apical side of each inserts were scraped off. Cells on the top of the chamber were removed and cells that invaded through the Matrigel were fixed with cold methanol, stained with DAPI, and counted. The total number of migrated cells was determined by light microscopy. One way Anova followed by Students t test was used to compare the effect of treatment to the control.

Xenograft experiments

All animal work was done at the Affiliated Hospital of Qingdao University (Qingdao, China) in accordance with federal, local, and institutional guidelines. Mice were kept in isolated ventilated cages, fed ad libitum in a 12/12 hours cycle of light and dark. 6 weeks Female nude mice (Animal Research Center, Shanghai, China) of age were used to generate the xenograft tumor models. $5x10^6$ [8505C/SW1736 (S100A4 shRNA or scramble shRNA) 8505C/SW1736] cells in 10 μL of serum-free RPMI medium were injected subcutaneously, respectively. 4-5 weeks after implantation for 8505C cells (3-4 weeks for SW1736 cells), when the average tumor volume reached approximately 100~ 250 mm^3 volume, the animals received either 120 mg/kg vemurafenib (oral gavage) or vehicle control (contained 3% DMSO and 1% methylcellulose) twice daily for 15 days as previously described [35]. Tumor size measurements and monitoring for signs of toxicity by body weight loss were performed at least twice a week. Tumor volume was calculated using the formula $V = (\pi/6)\times\text{length}\times\text{width}\times\text{height}$. Three hours after the last treatment, animals were sacrificed and tumors and lungs were removed and embedded into paraffin blocks. Formalin-fixed/paraffin-embedded lungs were cut at 5 μm thickness, sections were hematoxylin and eosin (H&E), stained and lung foci were counted. Standard hematoxylin and eosin (H&E) staining of paraffin-embedded tissue was performed for histological examination and analyzed by immunohistochemistry.

Histological and Immunohistochemical Analysis

Fresh tumors in each group were resected on three hours after the last treatment, fixed in formalin, embedded, cut, and mounted. Hematoxylin and eosin stained sections were evaluated by a pathologist in a blinded manner and processed for immunohistochemical analysis (IHC) according to the manufacturer's instructions. IHC was performed using Ki-67, S100A4, pAKT, and pERK antibodies. Annexin-V and terminal deoxynucleotidyl transferase-mediated dUTP nick-end labeling (TUNEL) assay was performed as described previously [36]. Positive cells with TUNEL staining were quantified from the average of three representative

high power fields (HPF, 200X) under light microscope. Stained and IHC tissue sections were visualized using a Nikon light microscope. Microscopic images were captured and processed using AxioCam digital microscope camera and AxioVision Image processing software (Olympus Corp., Lake Success, NY).

Statistical analysis

Statistical analysis was performed using the SPSS software, version 22.0. The results were expressed as the mean ± standard deviation. For *in vitro* experiments and animal studies, t-test or one-way ANOVA followed by a Bonferroni *post hoc* test was used to calculate the P values. A p-value ≤ 0.05 is considered to be statistically significant.

Results

Targeting S100A4 induces apoptosis and inhibits survival, migration and invasion of ATC cells

To determine the effect of S100A4 on ATCs, we first detected the S100A4 expression in the 4 ATC cell lines, 8505C $^{(BRAFV600E/mt)}$, SW1736 $^{(BRAFV600E/mt)}$, KAT18 $^{(BRAFV600E/wt)}$ and Cal-62$^{(BRAFV600E/wt)}$. We found that 8505C $^{(BRAFV600E/mt)}$ and Cal-62$^{(BRAFV600E/wt)}$ showed significantly higher baseline expression of S100A4 protein than the SW1736 and KAT18 cells (Fig. 1A). We used S100A4 shRNA and scrambled shRNA against S100A4 in 8505C and Cal-62 cells, and found 48 hs after transfection with S100A4 shRNA, but not with the scrambled shRNA, diminished S100A4 protein levels (Fig. 1B) in 8505C and Cal-62 cells.

Likewise, we used pCMV6-XL5-S100A4 cDNA (abbreviated as S100A4 cDNA) and control plasmid pCMV6-XL5 (empty vector) to transfected SW1736 and KAT18 cells (low endogenous S100A4), and found 48 hs after transfection with S100A4 cDNA upregulated S100A4 protein levels, compared to the empty vector transfection (Fig. 1C).

Compared to parental cells carrying empty vector (8505C –empty, Cal-62 empty), targeting endogenous S100A4 in 8505C cells and Cal-62 exhibited a growth inhibitory effect by MTT assays (Fig. 1D); Conversely, S100A4 overexpression in SW1736 and KAT18 significantly increased cell proliferation, leading to more than a 1.36-fold increase in cell number compared to vector controls after 3 days of culture (Fig. 1D). These results were consistent with the BrdU incorporation assays which showed that the percentage of BrdU positive cells was significantly decreased in S100A4 knockdown cells and significantly increased in S100A4-overexpressing cells (Fig. 1E). Similarly, flow cytometric analysis showed that significantly more apoptotic sub-G1 phase and annexin V positive cells were detected on S100A4 knockdown in both 8505C and Cal-62 cells (Fig. 1F-1G). Whereas S100A4 overexpression in SW1736 and KAT18 cells did not affect the sub-G1 phase and annexin V positive cells (Fig. 1F-1G).

The result from Matrigel invasion (Fig. 1H)and Transwell migration(Fig. 1I) assay indicated that S100A4 knockdown significantly inhibited invasion of 8505C cells and Cal-62 cells by 52%,40% and 56%,42%, respectively, as compared to scrambled shRNA transfected cells. However, S100A4 overexpression significantly increased the invasion of SW1736 and KAT18 cells by 48%, 53% and 43%, 48%, respectively, as compared to empty-vector transfected cells(Fig. 1H-1I).

Targeting S100A4 induces apoptosis and decreases invasion in ATC cells and is reversed by re-activation of AKT or /ERK or ROCK pathways

RhoA/ROCK, PI3K/Akt and Ras/MEK/ERK are three of the most frequently hyperactivated pathways in cancer cells. The S100A4 overexpression is known to signal via these signals, leading to enhanced invasion, proliferation and resistance to apoptosis. We then investigated the mechanisms by which targeting S100A4 blocks growth, migration and invasion of ATC cells.

The baseline expression of pAkt, pERK, RhoA/ROCK levels were detected in 8505C and Cal-62 cells by western blot assay. The 8505C and Cal-62 cells had rich expression of

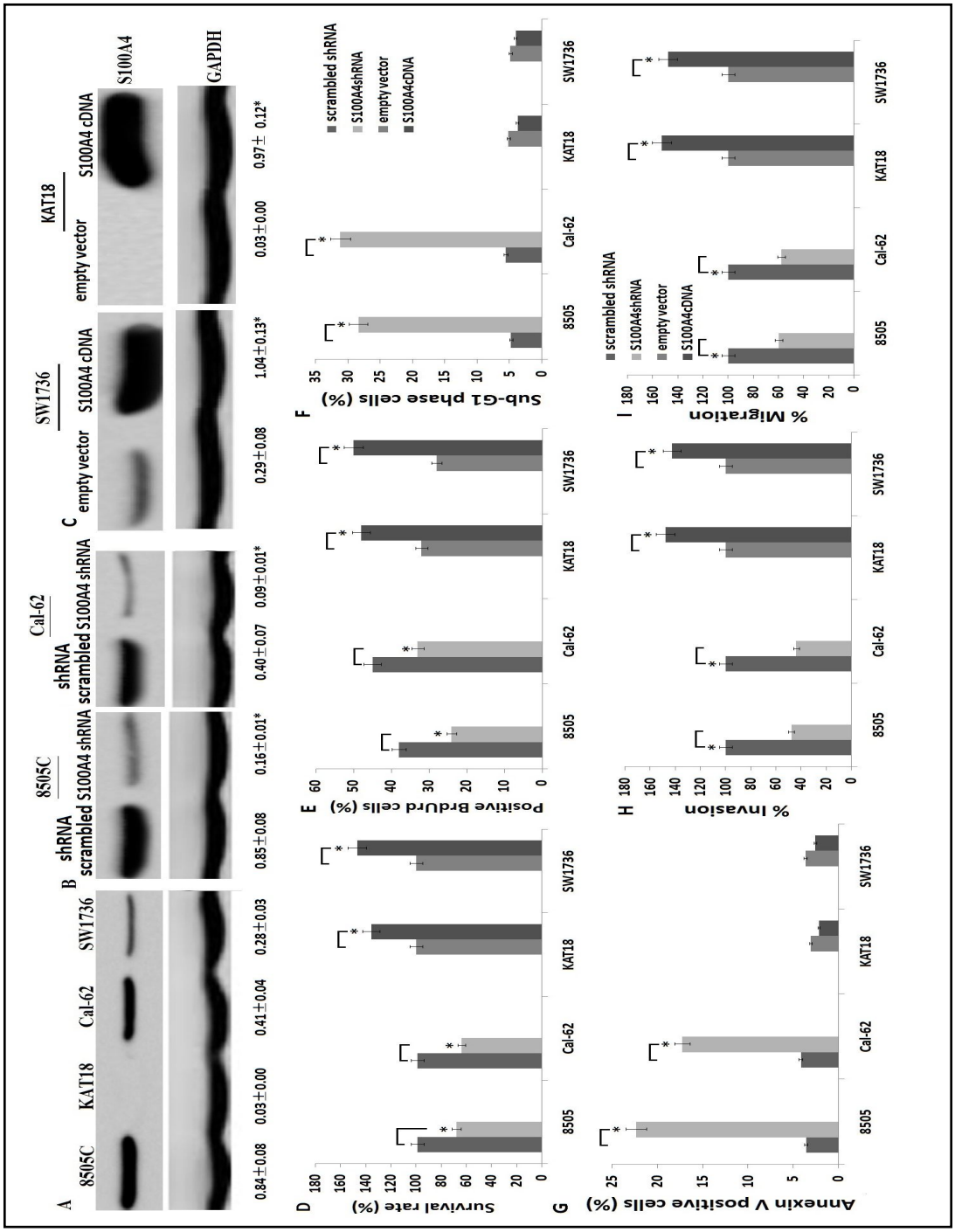

Fig. 1. Control of cell apoptosis, proliferation, invasion and migration by S100A4. A, Western blot analysis for endogenous S100A4 protein in 8505C, SW1736, KAT18 and Cal-62 cells; B, 8505C and Cal-62 cells were transfected with S100A4 shRNA or empty vector for 48 h, S100A4 protein was detected by Western blot assay. C, SW1736 and KAT18 cells were transfected with S100A4 cDNA and empty vector for 48 h, S100A4 protein expression was detected by Western blot assay. 8505C and Cal-62 cells were transfected with S100A4 shRNA for 48 h, and SW1736 and KAT18 cells were transfected with S100A4 cDNA for 48 h. MTT assay for cell survival(D); BrdUrd incubation for cell proliferation(E); Percentage of sub-G1 apoptotic phase cells(F); Annexin V positive apoptotic cells(G); Transwell migration assays(H); Matrigel invasion assay(I).*p<0.05.

baseline pAkt, pERK, RhoA/ROCK levels, which was blocked by S100A4 shRNA transfection in 8505C cells (8505C/ S100A4 shRNA) and Cal-62 cells (Cal-62/S100A4 shRNA) (Fig. 2A). We therefore investigated whether re-expressing these three pathways by using selectively overexpressed constitutively active forms of pCDNA-Myc-pERK, pCMV6-HA-Akt, pCMV-RhoA vector transfection may affect the sensitivity of 8505C and Cal-62 cells to S100A4 knockdown-induced apoptosis and invasion inhibition. As expected, transfection of the 8505C/S100A4 shRNA and Cal-62/S100A4 shRNA cells with these vector reversed the phosphorylation of pAkt, pERK, RhoA/ROCK in both of the cells (Fig. 2B).

The constitutively active forms of pCDNA-Myc-pERK and pCMV6-HA-Akt, but not pCMV-RhoA significantly reduced S100A4 knockdown-induced apoptosis of 8505C and Cal-62 cells (Fig. 2C-2D). Similar results were obtained using MTT cell survival assay (Fig. 2E) and BrdUrd incorporation assay (Fig. 2F). In addition, combined transfection of pCDNA-Myc-pERK and pCMV6-HA-Akt could not completely restored S100A4 knockdown-induced apoptosis and cell survival(data not shown).

In addition, the constitutively active forms of pCMV6-HA-Akt or pCMV-RhoA, not pCDNA-Myc-pERK significantly, but partly restored S100A4 knockdown-induced invasion and migration in 8505C and Cal-62 cells (Fig. 2G-2H). Furthermore, combined transfection of pCMV6-HA-Akt and pCMV-RhoA could not completely restored S100A4 knockdown-induced inhibition of invasion and migration (data not shown). These results suggest that S100A4 may be preferentially required for survival in ATC cells with higher activities of the Akt and ERK pathways, but required for invasion and migration with higher activities of the Akt and ROCK pathways.

S100A4 promotes proliferation and invasion in ATC cells and is reversed by inhibitors of AKT or ERK or RhoA/ROCK pathways

It has showed above that introduction of the S100A4 cDNA into SW1736 and KAT18 cells (low endogenous S100A4) accelerated their proliferation rate, migration, and invasion. We then investigated the mechanisms by which S100A4 promotes the effect in SW1736 and KAT18 cells. We found that S100A4 overexpression activated all the pAkt, pERK, RhoA/ROCK signaling (Fig. 3A). However, treatment of the S100A4 cDNA /SW1736 and S100A4 cDNA/ KAT18 cells with 10μM doses of inhibitors for 72 h (Y27632 or U0126 or MK-2206) inhibited phosphorylation of their corresponding downstream targets (data not shown). Y27632 treatment alone did not affect cell proliferation (Fig. 3B-3C) but partly reduced cell invasion (Fig. 3D) and migration (Fig. 3E). U0126 treatment alone did not affect cell invasion (Fig. 3D) and migration (Fig. 3E), but partly reduced cell proliferation (Fig. 3B). Treatment of MK-2206 alone partly reduced cell proliferation (Fig. 3B-3C), invasion (Fig. 3D) and migration (Fig. 3E). It was indicated that S100A4 promoted cell proliferation and growth mainly by activation of Akt and ERK pathways, and promoted invasion and migration mainly by activation of Akt and ROCK pathways.

S100A4 knockdown-vemurafenib combination treatment in 8505C and SW1736 cells

8505C and SW1736 cells were treated with vemurafenib (0.1μM, 1μM and 5μM) for 72 h. The cell viability *in vitro by* MTT *with* vemurafenib treatment for the 8505C and SW1736 *cells* are shown in Fig. 4A. Vemurafenib inhibited cell viability in dose-dependent manner in both 8505C and SW1736 *cells.* We then performed an apoptosis assay by flow cytometry using annexinV and Propidium Iodide (PI). Both of the cell lines showed no increased apoptosis (Fig. 4B). In addition, treatment of 8505C and SW1736 with vemurafenib increased invasion and migration rates (Fig. 4C-4D). *However*, when combined with S100A4 knockdown and vemurafenib treatment, cell apoptosis was significantly increased, and cell viability, invasion and migration was significantly decreased compared to the individual treatment (Fig. 4A-4D). Scrambled shRNA transfection has no effect on 8505C and SW1736 cells following vemurafenib treatment (data not shown).

It has shown that concentration of 2 μM was a clinically achievable blood and tissue concentration for vemurafenib [37]. So we used concentration of 2 μM of vemurafenib

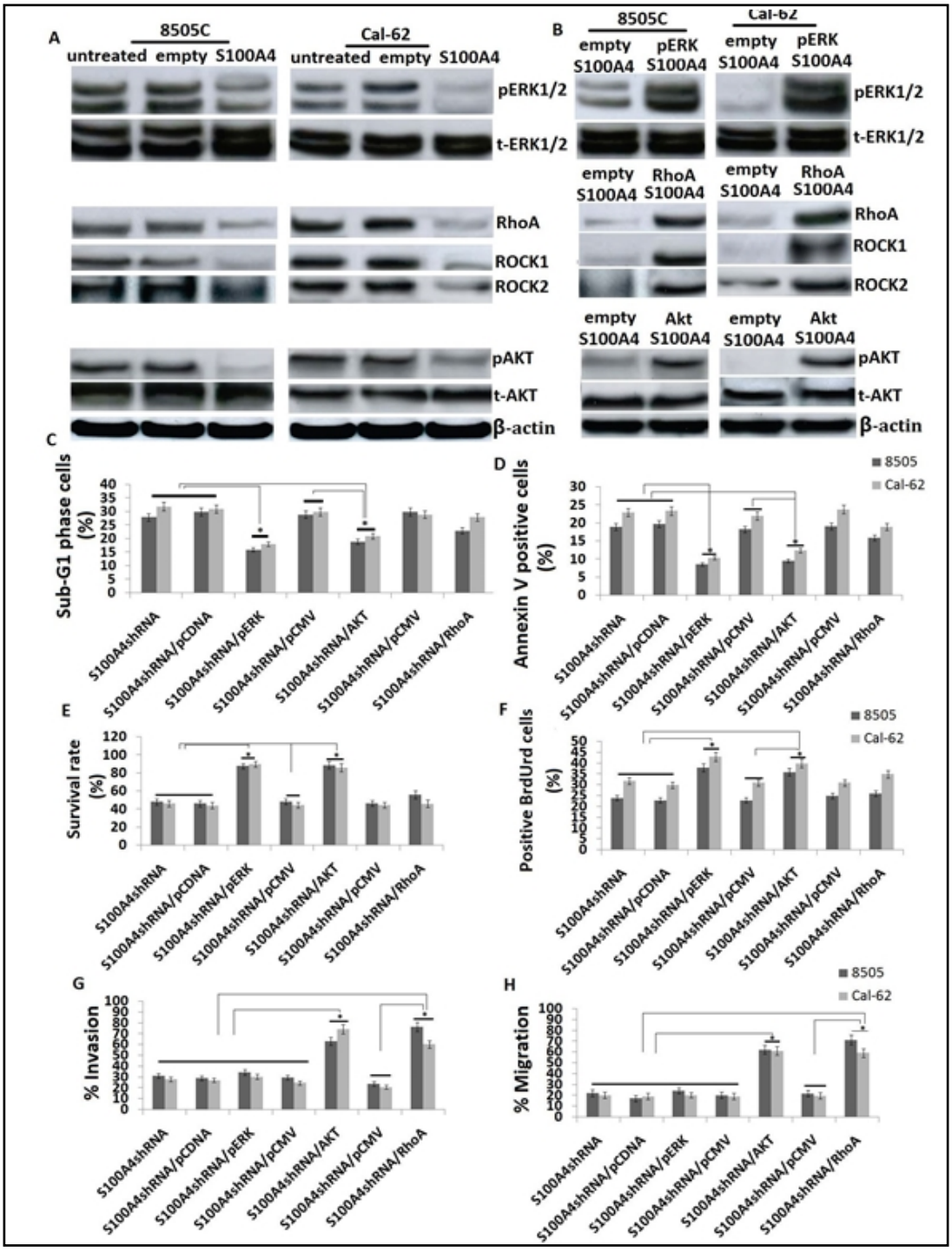

Fig. 2. Targeting S100A4 induces apoptosis and inhibits growth, invasion and migration to a different extent in different conditions. A, Western blot analysis for Akt or ERK, RhoA/ROCK signals in 8505C and Cal-62 cells after S100A4 knockdown. B, Western blots of Akt or ERK, RhoA/ROCK signals in 8505C/S100A4 shRNA and Cal-62/S100A4 shRNA cells transfected with pCDNA-Myc-pERK, pCMV6-HA-Akt, pCMV-RhoA vector at 48 hs post-infection. 8505C/S100A4shRNA and Cal-62/S100A4shRNA cells transfected with pCDNA-Myc-pERK, pCMV6-HA-Akt, pCMV-RhoA vector at 24 hs post-infection. Cells were harvested at 72 hours post-infection. Percentage of sub-G1 apoptotic phase cells(C); G, Annexin V positive apoptotic cells(D); MTT assay for cell survival(E); BrdUrd incubation for cell proliferation(F);Transwell migration assays(G); Matrigel invasion assay(H).*p<0.05.

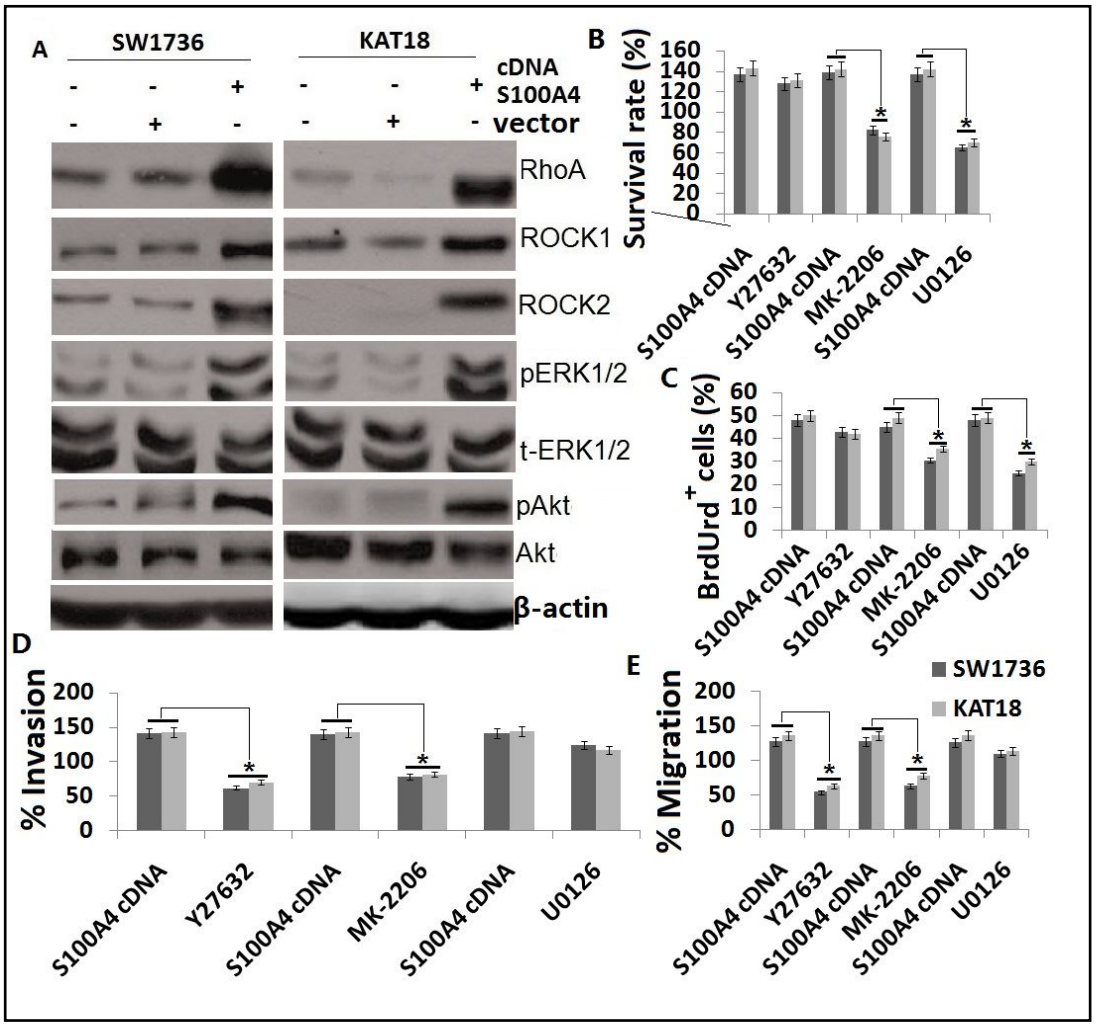

Fig. 3. S100A4 promotes growth, invasion and migration to a different extent in different conditions. A, Western blot analysis for Akt or ERK, RhoA/ROCK signals in SW1736 and KAT18 cells after S100A4 overexpression. B, S100A4 cDNA/SW1736 and S100A4 cDNA/KAT18 cells were treated with 10μM dose of inhibitors (Y27632 or U0126 or MK-2206) for 72 h, cell viability , proliferation, invasion and migration was detected by MTT(B), BrdUrd incubation (C), Matrigel invasion (D) and Transwell migration assays (E).*p<0.05.

treatment to understand the mechanism underlying the inhibition vemurafenib or/and S100A4 knockdown. Phosphorylation of ERK(p-ERK) is a key step down stream of BRAF and MEK in the signaling of the MAP kinase pathway and is widely used as a measure of the signaling activity of this pathway. We therefore examined the effect of the vemurafenib on the pERK in 8505C and SW1736 cell lines. As shown in Fig. 4E-4F in both 8505C and SW1736 cells, 2 μM of vemurafenib for 24 hs caused and maintained complete inhibition of BRAF. Vemurafenib at a concentration of 2 μM deminished pERK activity at early 2 hs, and reached the lowest at 4 h, then the pERK activity was gradually increased and reached the highest at 48 h (Fig. 4E-4F). And in the SW1736 cells, pERK activity was completely inhibited at early 2 hs, then gradually increased and reached the highest at 24h and maintained at 48hs (Fig. 4E-4F). Furthermore, we found that vemurafenib treatment gradually elevated p-Akt levels in both of the cells (Fig. 4E-4F). It is possible that this recovery from ERK activation inhibition or activation of AKT in both of the cells is related to the resistance of vemurafenib. Although ERK and AKT was activated with vemurafenib treatment in both of the cells, they were

completely blocked in combination with S100A4 knockdown and vemurafenib treatment in both of the cells (data not shown).

Vemurafenib treatment alone did not affect cell apoptosis, but inhibited cell growth in both of the 8505C and SW1736 cells. To understand the mechanism underlying the inhibition, we investigated the effect of vemurafenib on cell cycling. Upon cell cycle analysis, 76% and 80% of untreated 8505C and SW1736 cells were in S phase and 16% and 19% in G1/G0, indicative of rapid proliferative growth. However, treatment with vemurafenib caused 40% and 43% of cells arrested in G1/G0 and 36% and 39% in S phase with a significant increase in the G1/S ratio upon vemurafenib treatment in 8505C and SW1736 cells, respectively. Therefore, the inhibition of 8505C and SW1736 cell growth by vemurafenib was mainly through cell cycle arrest but not cell apoptosis.

We evaluated whether vemurafenib inhibited growth of 8505C and SW1736 cells by inactivation of pERK.

As shown in Fig. 4G, vemurafenib inhibited pERK in both of the cells, and vemurafenib treatment inhibited tumor cell viability and proliferation, but produced relatively minimal effects when 8505C and SW1736 cells were treated with combined vemurafenib 2μM and 10μM dose of U0126 for 72 h (Fig. 4H-4I).

To confirm that pAKT activation drives vemurafenib resistance in 8505C and SW1736 cells, 8505C and SW1736 cells were treated with combined vemurafenib 2μM and 10μM dose of MK-2206 for 72 h and measured their rate of viability and proliferation. As shown in Fig. 4G, vemurafenib inhibited pAKT in both of the cells, and combined treatment was significantly reversed cell viability and proliferation in vemurafenib alone treated 8505C and SW1736 cells(Fig. 4H-4I). In addition, combined treatment was significantly reverse cell viability and proliferation in S100A4 shRNA treated 8505C and SW1736 cells (Fig. 4H-4I). These results confirmed that activation of pERK and pAKT makes 8505C and SW1736 cells require resistance. Furthermore, S100A4 knockdown sensitized 8505C and SW1736 cells to vemurafenib-induced growth inhibition by inhibition of pERK and pAKT.

We next evaluated whether vemurafenib promoted invasion and migration in 8505C and SW1736 cells by activation of pERK and pAKT. As shown in Fig. 4J-4K, combined vemurafenib and U0126 produced relatively minimal effects on vemurafenib-induced invasion and migration. Whereas combined vemurafenib and MK-2206 treatment produced significant inhibition effects on vemurafenib-induced invasion and migration, indicating that vemurafenib promoted invasion and migration by mainly activation of pAKT signals in 8505C and SW1736 cells.

S100A4 knockdown enhances the antitumor effect of vemurafenib in vivo

To confirm our *in vitro* observations *in vivo*, the mice bearing palpable 8505C or SW1736 tumors, S100A4 shRNA/vehicle transfected 8505C or SW1736 tumors receive vemurafenib treatment. Due to a lack of toxicity, a maximum tolerable dose for PLX4032 was not reached in mice. Yang et al. [35] selected a dose of 100 mg/kg bid was as the highest dose to be tested in efficacy studies. In our pre-experiment, no significant improvement of the therapeutic effect was noted at 120 mg/kg with respect to 240 mg/kg, indicating that maximal therapeutic efficacy was already achieved at 120 mg/kg. So we selected a dose of 120 mg/kg bid for further study.

Vemurafenib treatment alone inhibited tumor growth, but the difference was not significant, suggested that vemurafenib alone was partly susceptible to tumor growth (Fig. 5A-5B). In addition, S100A4 shRNA/8505C tumors grew slowly relative to the untreated, but the difference in growth between S100A4 shRNA/tumors and untreated tumor was not significant, suggested that S100A4 shRNA alone has part of the effect on tumor growth in 8505C cells (Fig. 5A). S100A4 shRNA had no effect on SW1736 tumors growth (Fig. 5B). Consistent with results obtained in cultured cells, we observed a dramatic response to combined S100A4 shRNA and Vemurafenib treatment. Combination-treated animals exhibited an enhanced tumor response (Fig. 5A-5B). In addition, the body weight of the treated mice was not significantly different from that of the control mice.

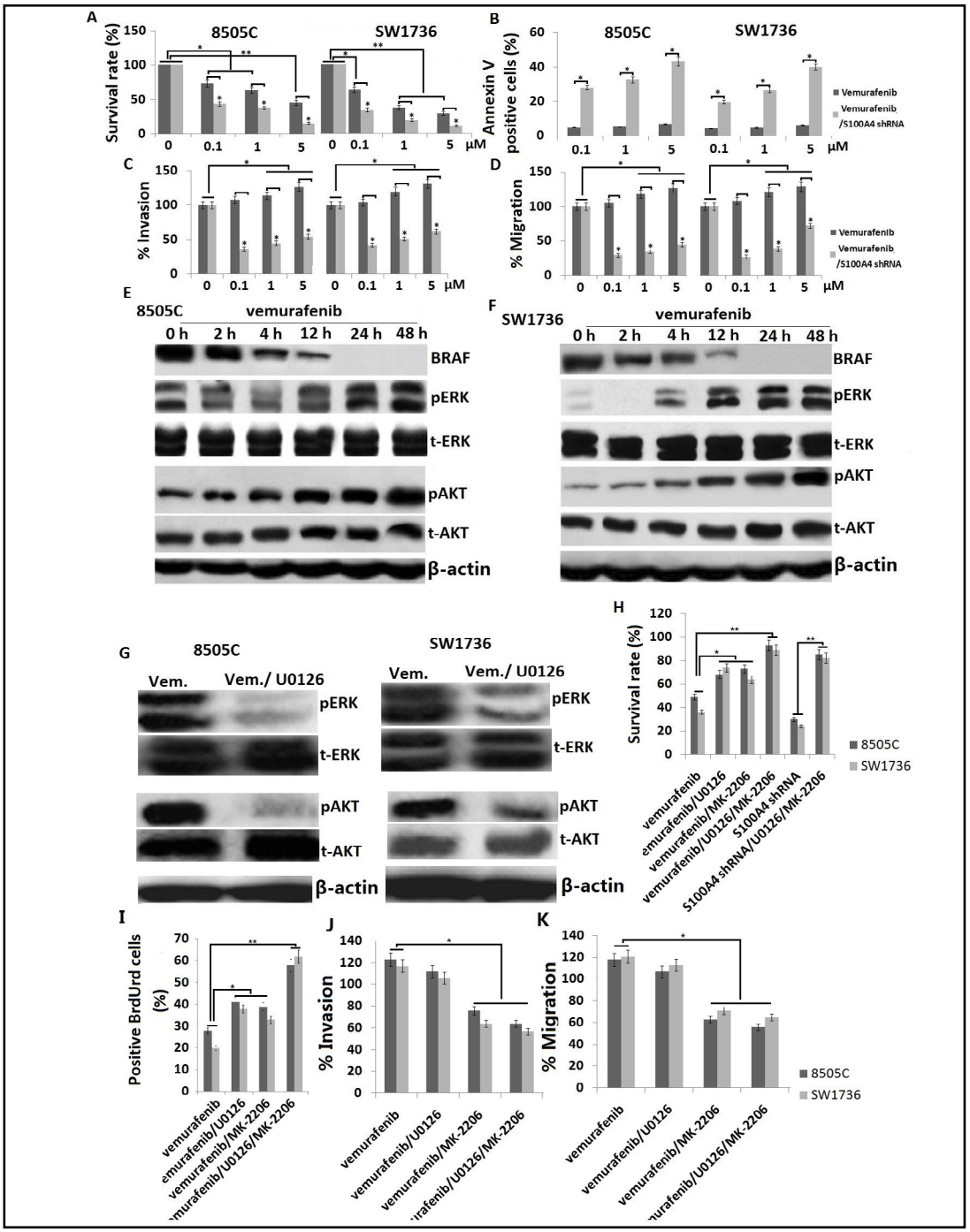

Fig. 4. S100A4 knockdown sensitizes 8505C and SW1736 cells to vemurafenib in vitro.shRNA knockdown of S100A4 in the presence of 0.1,1,5.0 μM vemurafenib for 72 h. Cell viability was detected by MTT assay(A); Proliferation was detected by BrdUrd incubation assay(B);Invasion by Matrigel invasion assay(C) and Migration by Transwell migration assays (D). 8505C and SW1736 cells were treated with 2.0 μM vemurafenib for 2-48 h, different protein expression was detected by Western blot assay (E-F); 8505C and SW1736 cells were treated with 2.0 μM vemurafenib or/and 10μM U0126 or/and 10μM MK-2206 for 48 h. pERK and pAKT was detected by Western blot assay(G). 8505C and SW1736 cells were treated with 2.0 μM vemurafenib or/and in combination with 10μM U0126 or/and 10μM MK-2206 or /and S100A4 shRNA for 72 h. Cell viability was detected by MTT assay(H); Proliferation was detected by BrdUrd incubation assay(I);Invasion by Matrigel invasion assay(J) and Migration by Transwell migration assays (K).$^{**}P<0.05$;$^{**}P<0.01$.

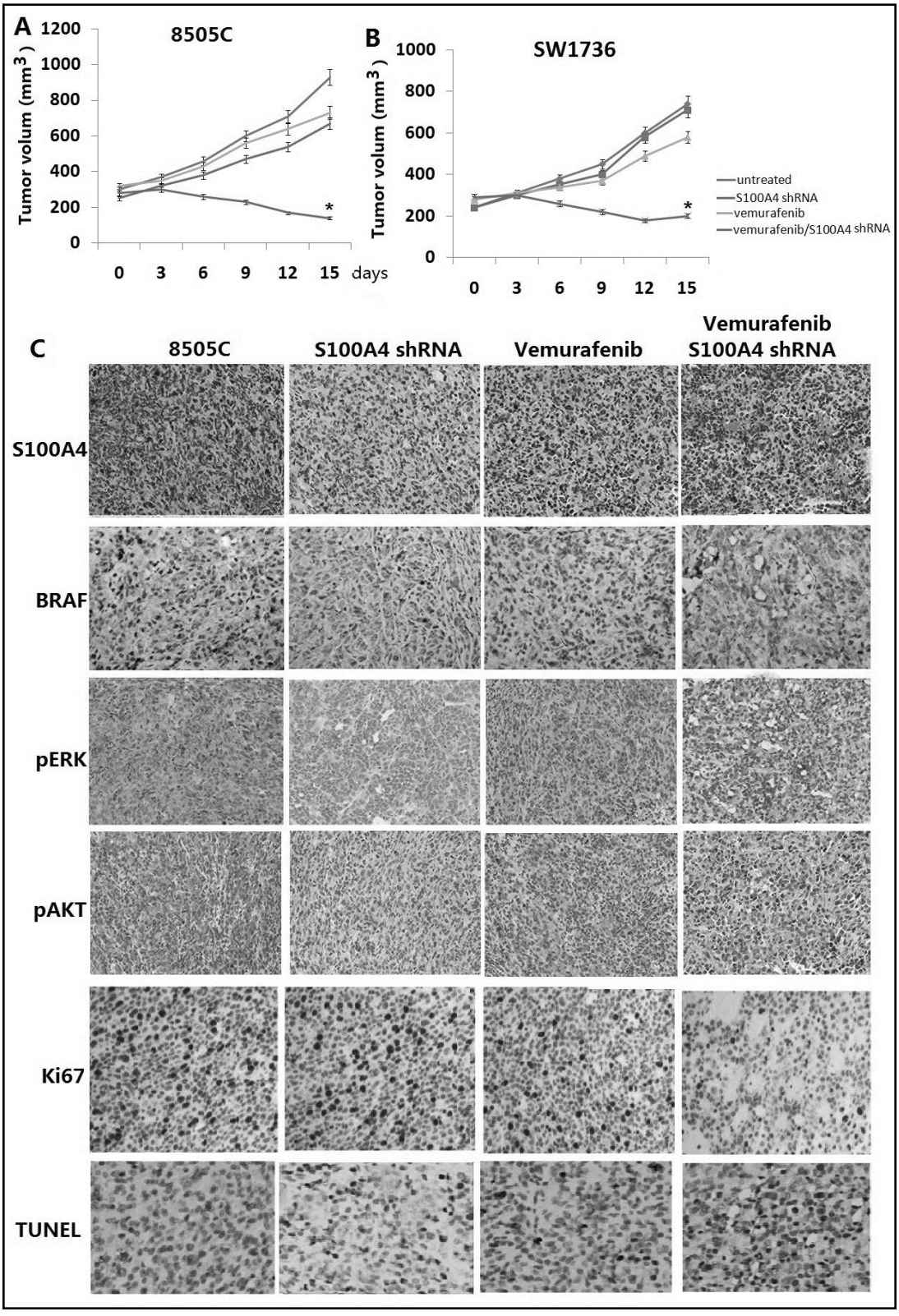

Fig. 5. In vivo therapeutic efficacy of S100A4 shRNA in combination with Vemurafenib. Combined S100A4 shRNA and Vemurafenib results in synergistic reduction in growth **of** 8505C and SW1736 tumors in vivo (A and B).immunohistochemistry (IHC) assay for BRAF, S100A4, pAKT, pERK, Ki67 and TUNEL staining in vivo tumors (C).*P<0.01.

To further assess proliferation and apoptosis in 8505C tumors *in vivo*, Ki-67 and TUNEL immunohistochemistry was performed. We observed a significant decrease in the proliferation index (stained nuclei per field) from 64.6% ± 9% in untreated tumors to 8.6 ± 2.8% in combination of S100A4 shRNA and vemurafenib treated tumors (Fig. 5C). S100A4 shRNA or vemurafenib alone led to a lower proliferation index decrease than combined treatment (Fig. 5C). TUNEL staining revealed a significant increase of apoptotic cells in the combine treated mice compared to the S100A4 shRNA or vemurafenib alone. Finally, we analyzed the gene expression of S100A4, BRAF, pERKT and pAKT of response to vemurafenib or/and S100A4 shRNA treatment. As shown in Fig. 5C, tumor growth inhibition was associated with a remarkable reduction of nuclear reactivity for pERK or/and pAkt in both vemurafenib and S100A4 knockdown combination treatment in 8505C tumors (Fig. 5C) compared to the vemurafenib or S100A4 shRNA treatment alone. Vemurafenib and S100A4 knockdown combination treatment in SW1736 cells has the same results as that in 8505C tumor *in vivo* (data not shown).

We planned to investigate the effect of vemurafenib or/and S100A4 knockdown combination treatment on lung metastases of our models with subcutaneous approaches, but we did not detect the presence of pulmonary metastases in untreated model within 5-6 weeks, indicating that subcutaneous approaches is not easy to construct lung metastases of our models. Therefore we have not assessed the response of vemurafenib or/and S100A4 knockdown combination on lung metastases of our models.

Discussion

Potent inhibitors of $BRAF^{V600E}$, such as vemurafenib, show great promise for treatment of $BRAF^{V600E}$-positive thyroid cancer. However, the rapid development of acquired resistance presents a significant therapeutic challenge to cancer patients receiving vemurafenib [38]. Single-compound approaches might fail in treating aggressive thyroid tumors, which depending on more than one altered pathway (and/or rapidly develop resistance via feedback mechanisms [39, 40]. For example, vemurafenib showed transient growth inhibition in thyroid cancer cells via targeting MEK1/2-ERK1/2 signal and quickly developed resistance via activation of ErbB/HER pathway [39]. However, the combined treatment of MAP-ERK kinase inhibitors and HER kinase inhibitor sensitizes BRAF-mutant thyroid cancer cells [39]. Similar synergistic effects were observed in others studies targeting MAPK and AKT pathways in thyroid cancer cell lines harboring both the activating $BRAF^{V600E}$ and PIK3CA mutations [41], suggesting that combinatorial therapies are expected to be more successful in treating aggressive thyroid cancers.

Previously studies have shown that PIK3CAH1047R mutations and BRAFV600E collaborate to promote rapid PTC formation and eventual ATC progression. Therefore, targeting both the Pi3′-kinase→AKT→mTOR and RAF→MEK→ERK pathways is a good rational to tackle aggressive forms of thyroid cancer.

S100A4 is not only a metastatic protein but also an oncoprotein that plays a critical role in the development of tumors. Depletion of S100A4 resulted in impaired proliferation and invasive capacity, including thyroid cancer [17, 21, 42], suggesting the importance of S100A4 in progressive phenotypes of cancers. Our *in vitro* study showed that targeting S100A4 in 8505C and Cal-62 cells decreases cell proliferation, invasion and migration and increases cell apoptosis. Whereas, S100A4 overexpression promotes cell proliferation, invasion and migration, but not affect cell apoptosis in SW1736 and KAT18 cells. Our *in vitro* findings are consistent with previous *in vitro* studies [17].

The PI3K/AKT pathway, often activated in thyroid cancer, has a fundamental role in thyroid tumorigenesis [43, 44]. This signaling pathway regulates cell growth and proliferation, cell motility, survival, and be as a therapeutic target in human cancers have been extensively investigated [45, 46]. Normal MAPK/ERK function is responsible for tumor suppression through induction of senescence and ubiquitinization and degradation of proteins necessary

for cell cycle activity and survival. ERK phosphorylation results in the activation of multiple substrates that are responsible for stimulation of cell proliferation [47]. In our study, AKT and ERK was activated in 8505C and Cal-62 cells. In S100A4 knockout 8505C and Cal-62 cells, AKT and ERK phosphorylation was inhibited, followed by defective proliferation, invasion, migration and increased apoptosis. To test the possibility that S100A4 knockout on these effect is associated with the inactivation of AKT and ERK signaling pathway, the constitutively active forms of pCDNA-Myc-pERK and pCMV6-HA-Ak were employed. We observed that restoration of AKT alone or ERK alone significantly, but partly, reversed the anti-proliferation and pro-apoptosis effect. Furthermore, combined treatment of pCDNA-Myc-pERK and pCMV6-HA-Akt could not completely restored the effect of S100A4 knockout. We also observed that restoration of AKT alone significantly, but partly, reversed the anti-metastatic effect. Whereas, restoration of ERK alone could not reversed the anti-metastatic effect, suggesting that there are other S100A4-regulated signals took part in the regulation of cell growth and invasion.

To test the possibility that S100A4 overexpression on these effect is associated with the activation of AKT and ERK in SW1736 and KAT18 cells, 10μM doses of inhibitors (U0126 or MK-2206) was used. We observed that S100A4 overexpression increased the phosphorylation of ERK and AKT, followed by increased proliferation, invasion and migration of SW1736 and KAT18 cells. However, preincubation of the cells with the U0126 or/and MK-2206 resulted in only minimal residual ERK and AKT-phoshorylation, and reduced the proliferation effect.

ROCK, which exists in two isoforms, ROCK1 and ROCK2, is a downstream effector of RhoA. It was reported that ROCK is critical in controlling migration, proliferation, cell apoptosis/survival, gene transcription and differentiation [48]. A recent study showed that RhoA signal could be regulated by S100A4 [49]. In the present study, we found that RhoA/ROCK1/2 was activated in 8505C and Cal-62 cells, S100A4 knockout reduced RhoA/ROCK1/2 expression. Restoration of RhoA/ROCK1/2 by constitutively active forms of pCMV-RhoA significantly reversed the anti-metastasis effect of S100A4 knockout. But restoration of RhoA/ROCK1/2 did not affect cell proliferation and apoptosis of S100A4 knockout cells. RhoA/ROCK1/2 was activated in the SW1736 and KAT18 cells overexpressing S100A4. 10μM doses of ROCK2 inhibitors Y27632 was sufficient to inhibited invasion and migration, but proliferation and apoptosis of SW1736 and KAT18 cells overexpressing S100A4 was not affected. These results suggest that S100A4 may be preferentially required for survival in ATC cells with higher activities of the Akt and ERK pathways, but required for invasion and migration with higher activities of the Akt and ROCK pathways. Therefore, targeting S100A4, resulted in AKT, ERK and ROCK signals inactivation, inhibited cell proliferation and metastasis.

Vemurafenib is the selective RAF inhibitor that was used for patients with $BRAF^{V600E}$ metastatic melanoma. However, resistance to $BRAF^{V600E}$ inhibitors has recently emerged as a major therapeutic challenge in eradicating melanoma [50]. Furthermore, the majority of BRAF-mutant thyroid cancer cell lines have proven to be resistant to vemurafenib, and the reason for this disparity remains unclear.

In our study, we found that Vemurafenib treatment inhibited 8505C and SW1736 cell proliferation and caused cell cycle arrest in a dose-dependent way. But it did not affect cell apoptosis, indicating Vemurafenib inhibited cell proliferation by cell cycle arrest. In addition, Vemurafenib did not inhibit invasion and metastasis of 8505C and SW1736 cell, but enhanced this effect, resulting in no further clinical benefit of the drug. This was not rather expected. Previous study has reported that the stromal cell secretion of hepatocyte growth factor (HGF) confers resistance to BRAF inhibitor therapy by activation of the MAPK and the PI3K/AKT signaling, and reversed this resistance by combining a BRAF inhibitor with HGF and/or HGF receptor (MET) inhibitor [51]. Recent study has reported that Vemurafenib treatment significantly increased levels of p-AKT, which made the cells acquired the resistance to Vemurafenib [52]. In our study, pERK levels was significantly reduced at 2-4 h after Vemurafenib treatment, then the pERK levels was gradually increased and reached the highest levels at 48 h for both of the 8505C and SW1736 cells. Furthermore, p-Akt levels in both of the cells was gradually increased and reached the highest levels at

24h and maintained at 48 hs. Jin et al. [41] has found that combined targeting of ERK and PI3K signaling potently inhibits growth in preclinical models in thyroid cancer. We next determined whether targeting ERK and PI3K signaling resulted in the same results. The 8505C and SW1736 cells treated with vemurafenib/U0126 or vemurafenib/MK-2206 or vemurafenib/U0126/MK-2206 for 72h resulted in the blockage of ERK and PI3K expression, and reversed the cell viability and proliferation, and confirmed that activation of pERK and pAKT makes 8505C and SW1736 cells require resistance. In addition, 8505C and SW1736 cells treated with vemurafenib /MK-2206, but not vemurafenib/U0126 reversed the cell invasion and migration, suggesting that activation of pAKT promoted cell invation in vemurafenib-treated cells. The former has proved that targeting S100A4 could efficiently block pAKT and pERK expression. In our study, combined S100A4 knockout and vemurafenib treatment completely blocked the re-activation of pAKT and pERK in 8505C and SW1736 cells *in vitro*. Furthermore, systemic vemurafenib in combination with S100A4 knockout treatment resulted in enhanced antitumor activity vs vemurafenib or S100A4 *in vitro* alone.

Vemurafenib was shown to be effective in most metastatic melanoma patients with the $BRAF^{V600E}$ mutation [53]. Vemurafenib has been also used in a patient with ATC ($BRAF^{V600}$E mutation) for 28 days, resulted in nearly complete clearing of metastatic disease [14]. In addition, responses in ATC patients treated with vemurafenib have exhibited modest activity [15]. We used the subcutaneous approaches to construct Xenograft of 8505C and SW1736 cells and study the effect of Vemurafenib on Xenograft tumors. Our implantation of human 8505C ATC cells into SCID mice leads to the formation of thyroid tumors (100–250 mm^3) within four to five weeks post-implantation simple to the previous reports [54, 55]. The SW1736 cells need 3-4 weeks to form the thyroid tumors (100–250 mm^3). After 120 mg/kg vemurafenib treatment twice daily for 15 days, tumor size was decreased in both of the model as compared to vehicle treatment, however, there's no difference between the two groups, indicating that vemurafenib alone could not significantly enhance antitumor activity.

S100A4 has found to induce migration and invasion *in vitro* and metastasis *in vivo* in human colon cancer cell lines and tumors [56]. In prostate cancer (CaP) cells, S100A4-siRNA-transfected cells exhibited a reduced rate of tumor growth under *in vivo* conditions [17]. In our study, we observed that S100A4-shRNA-transfected 8505C cells with high S100A4 expression exhibited a less reduced rate of tumor growth *in vivo* as compared to vehicle treatment; In the S100A4-shRNA-transfected SW1736 cells with low S100A4 expression, no significant growth inhibition was observed as compared to vehicle treatment. It is suggested the targeting S100A4 alone could not significantly inhibit ATC tumors *in vivo*. However, combined treatment of S100A4-shRNA and vemurafenib resulted in more enhanced antitumor compared to the treatment alone in this preclinical model.

To further determine the mechanism by which S100A4-shRNA alone or vemurafenib alone or combination treatment on Xenograft tumor growth, we first detected the cellular signaling in Vemurafenib -treated vs. untreated by IHC in dissected tumor specimens. Vemurafenib treated tumors exhibited negative BRAF staining, positive pErk and pAKT staining, suggesting that pErk and pAKT was not completely inhibited to vemurafenib in 8505C and SW1736 tumors. However, pErk and pAKT staining was negative in S100A4shRNA alone and S100A4shRNA/vemurafenib treated tumors. In addition, combined treatment of S100A4shRNA and S100A4shRNA

results in a synergistic increase in TUNEL-positive cells and decrease in percentage Ki-67-positive cells. Therefore, combined treatment inhibits ERK1/2 and AKT activation following vemurafenib treatment and reversed the vemurafenib resistance. This therapeutic combination may be of benefit in patients with ATC.

Previous study has found that Vemurafenib treatment inhibited lung metastasis in metastatic melanoma [50]. But in our study, subcutaneous approaches could not produce lung metastasis model likely because of ectopic anatomical context. This was consistent with the previous report [57]. Many studies have reported that only orthotopic models could recapitulate metastatic behavior with sufficient penetrance and reproducibility [57, 58]. However, whether 8505C and SW1736 cells could produce orthotopic metastasis models,

and whether Vemurafenib or/and S100A4 shRNA has orthotopic anti-metastasis ability *in vivo* need further investigation in the future.

Conclusion

In summary, targeting S100A4 inhibits tumor growth in ATC *in vitro*, which could be mainly due to apoptosis associated with ERK1/2 and AKT signaling inactivation. Targeting S100A4 also inhibits tumor invasion and migration in ATC *in vitro*, which could be mainly associated with RhoA/ROCK and AKT signaling inactivation. Vemurafenib treatment inhibits cell viability and proliferation, but promotes cell invasion and migration *in vitro*.

Vemurafenib alone did not blocks tumor growth *in vivo*. Vemurafenib activates ERK1/2 and AKT signaling and makes the ATC cells resistant to Vemurafenib treatment. Combined treatment with S100A4 knockout and Vemurafenib reversed the vemurafenib resistance by inactivation of ERK1/2 and AKT signaling *in vitro and in vivo*. The data provide further evidence that targeting of targeting S100A4 is an attractive therapeutic strategy for ATC cells to sensitize vemurafenib treatment. In this context, genetic-guided combinational use of S100A4 knockout and vemurafenib may prove to be a particularly effective treatment for this cancer, which warrants a clinical trial.

Disclosure Statement

The authors declare that no conflict of interests exist.

References

1 Parkin DM, Bray F, Ferlay J, Pisani P: Global cancer statistics, 2002. CA Cancer J Clin 2005;55:74-108.
2 Neff RL, Farrar WB, Kloos RT, Burman KD: Anaplastic thyroid cancer. Endocrinol Metab Clin North Am 2008;37:525-538.
3 Kitamura Y, Shimizu K, Nagahama M, Sugino K, Ozaki O, Mimura T, Ito K, Ito K, Tanaka S: Immediate causes of death in thyroid carcinoma: clinicopathological analysis of 161 fatal cases. J Clin Endocrinol Metab 1999; 84:4043-4049.
4 Xing M: BRAF mutation in papillary thyroid cancer: pathogenic role, molecular bases, and clinical implications. Endocr Rev 2007;28:742-762 .
5 Xing M: Genetic alterations in the phosphatidylinositol-3 kinase/Akt pathway in thyroid cancer. Thyroid 2010;20:697-706.
6 Liu Z, Hou P, Ji M, Guan H, Studeman K, Jensen K, Vasko V, El-Naggar AK, Xing M: Highly prevalent genetic alterations in receptor tyrosine kinases and phosphatidylinositol 3-kinase/akt and mitogen-activated protein kinase pathways in anaplastic and follicular thyroid cancers. J Clin Endocrinol Metab 2008;93:3106-3116.
7 Nucera C, Porrello A, Antonello ZA, MekelM, NehsMA, Giordano TJ, Gerald D, Benjamin LE, Priolo C, Puxeddu E, Finn S, Jarzab B, Hodin RA, Pontecorvi A, Nose V, Lawler J, Parangi S: B-Raf(V600E) and thrombospondin-1 promote thyroid cancer progression. Proc Natl Acad Sci USA 2010;107:10649-10654.
8 Schweppe RE, Kerege AA, Sharma V, Poczobutt JM, Gutierrez-Hartmann A, Grzywa RL, Haugen BR: Distinct genetic alterations in the mitogen-activated protein kinase pathwaydictate sensitivity of thyroid cancer cells to mitogen-activated protein kinase kinase 1/2 inhibition. Thyroid 2009;19:825-835.
9 Salvatore G, De Falco V, Salerno P, Nappi TC, Pepe S, Troncone G, Carlomagno F, Melillo RM, Wilhelm SM, Santoro M: BRAF is a therapeutic target in aggressive thyroid carcinoma. Clin Cancer Res 2006;12:1623-1629.
10 Liu Y, Gunda V, Zhu X, Xu X, Wu J, Askhatova D, Farokhzad OC, Parangi S, Shi J: Theranostic near-infrared fluorescent nanoplatform for imaging and systemic siRNA delivery to metastatic anaplastic thyroid cancer. Proc Natl Acad Sci U S A 2016;113:7750-7755.

11 Nucera C, Nehs MA, Nagarkatti SS, Sadow PM, Mekel M, Fischer AH: Targeting BRAFV600E with PLX4720 displays potent antimigratory and anti-invasive activity in preclinical models of human thyroid cancer. Oncologist 2011;16:296-309.
12 McFadden DG, Vernon A, Santiago PM, Martinez-McFaline R, Bhutkar A, Crowley DM, McMahon M, Sadow PM, Jacks T: p53 constrains progression to anaplastic thyroid carcinoma in a Braf-mutant mouse model of papillary thyroid cancer. Proc Natl Acad Sci U S A 2014;111:E1600-1609.
13 Nehs MA, Nucera C, Nagarkatti SS: Late intervention with anti-BRAF(V600E) therapy induces tumor regression in an orthotopic mouse model of human anaplastic thyroid cancer. Endocrinology 2012;153:985-994.
14 Rosove MH, Peddi PF, Glaspy JA: BRAF V600E inhibition in ATC. N Engl J Med 2013;368:684-685.
15 Kim KB, Cabanillas ME, Lazar AJ, Williams MD, Sanders DL, Ilagan JL, Nolop K, Lee RJ, Sherman SI: Clinical responses to vemurafenib in patients with metastatic papillary thyroid cancer harboring BRAF(V600E) mutation. Thyroid 2013;23:1277-1283.
16 Poulikakos PI, Zhang C, Bollag G, Shokat KM, Rosen N: RAF inhibitors transactivate RAF dimers and ERK signalling in cells with wild type BRAF. Nature 2010;464:427-430.
17 Saleem M, Kweon MH, Johnson JJ, Adhami VM, Elcheva I, Khan N, Bin Hafeez B, Bhat KM, Sarfaraz S, Reagan-Shaw S,Spiegelman VS, Setaluri V, Mukhtar H: S100A4 accelerates tumorigenesis and invasion of human prostate cancer through the transcriptional regulation of matrix metalloproteinase 9. Proc Natl Acad Sci U S A 2006;103:14825-14830.
18 Mahon PC, Baril P, Bhakta V, Chelala C, Caulee K, Harada T, Lemoine NR: S100A4 contributes to the suppression of BNIP3 expression, chemoresistance, and inhibition of apoptosis in pancreatic cancer. Cancer Res 2007;67:6786-6795.
19 Ismail TM, Zhang S, Fernig DG, Gross S, Martin-Fernandez ML, See V, Tozawa K, Tynan CJ, Wang G, Wilkinson MC, Rudland PS, Barraclough R: Self-association of calcium-binding protein S100A4 and metastasis. J Biol Chem 2010;285:914-922.
20 Lo JF, Yu CC, Chiou SH, Huang CY, Jan CI, Lin SC, Liu CJ, Hu WY, Yu YH: The epithelial-mesenchymal transition mediator S100A4 maintains cancer-initiating cells in head and neck cancers. Cancer Res 2011;71:1912-1923.
21 Ismail TM, Bennett D, Platt-Higgins AM, Al-Medhity M, Barraclough R, Rudland PS: S100A4 Elevation Empowers Expression of Metastasis Effector Molecules in Human Breast Cancer. Cancer Res 2017;77:780-789.
22 Sun X, Wang Y, Zhang J, Tu J, Wang XJ, Su XD, Wang L, Zhang Y: Tunneling-nanotube direction determination in neurons and astrocytes. Cell Death Dis 2012;3:e438.
23 Grigorian M, Andresen S, Tulchinsky E, Kriajevska M, Carlberg C, Kruse C, Cohn M, Ambartsumian N, Christensen A,Selivanova G, Lukanidin E: Tumor suppressor p53 protein is a new target for the metastasis-associatedMts1/S100A4 protein: functional consequences of their interaction. J Biol Chem 2001;276:22699-22708.
24 Hyman DM, Puzanov I, Subbiah V, Faris JE, Chau I, Blay JY, Wolf J, Raje NS, Diamond EL, Hollebecque A, Gervais R, Elez-Fernandez ME, Italiano A, Hofheinz RD, Hidalgo M, Chan E, Schuler M, Lasserre SF, Makrutzki M, Sirzen F et al.: Vemurafenib in multiple nonmelanoma cancers with BRAF V600 mutations. N Engl J Med 2015;373:726-736.
25 Liu S, Li L, Zhang Y, Zhang Y, Zhao Y, You X, Lin Z, Zhang X, Ye L: The oncoprotein HBXIP uses two pathways to up-regulate S100A4 in promotion of growth and migration of breast cancer cells. J Biol Chem 2012; 287:30228-30239.
26 Boussemart L, Malka-Mahieu H, Girault I, Allard D, Hemmingsson O, Tomasic G, Thomas M, Basmadjian C, Ribeiro N, Thuaud F, Mateus C, Routier E, Kamsu-Kom N, Agoussi S, Eggermont AM, Désaubry L, Robert C, Vagner S: eIF4F is a nexus of resistance to anti-BRAF and anti-MEK cancer therapies. Nature 2014;513:105-109.
27 Meireles AM, Preto A, Rocha AS, Rebocho AP, Maximo V, Pereira-Castro I, Moreira S, Feijao T, Botelho T, Marques R, Trovisco V, Cirnes L, Alves C, Velho S, Soares P, Sobrinho-Simoes M: Molecular and genotypic characterization of human thyroid follicular cell carcinoma-derived cell lines. Thyroid 2007;17:707-715.
28 Lee JJ, Foukakis T, Hashemi J, Grimelius L, Heldin NE, Wallin G, Rudduck C, Lui WO, Hoog A, Larsson C: Molecular cytogenetic profiles of novel and established human anaplastic thyroid carcinoma models. Thyroid 2007;17:289-301.

29 Schweppe RE, Klopper JP, Korch C, Pugazhenthi U, Benezra M, Knauf JA, Fagin JA, Marlow LA, Copland JA, Smallridge RC, Haugen BR: Deoxyribonucleic acid profiling analysis of 40 human thyroid cancer cell lines reveals cross-contamination resulting in cell line redundancy andmisidentification. J Clin Endocrinol Metab 2008;93:4331-4341.
30 Zhao S, Venkatasubbarao K, Lazor JW, Sperry J, Jin C, Cao L, Freeman JW: Inhibition of STAT3 Tyr705 phosphorylation by Smad4 suppresses transforming growth factor beta-mediated invasion and metastasis in pancreatic cancer cells. Cancer Res 2008; 68:4221-4228.
31 Diep CH, Munoz RM, Choudhary A, Von Hoff DD, Han H: Synergistic effect between erlotinib and MEK inhibitors in KRAS wild-type human pancreatic cancer cells. Clin Cancer Res 2011;17:2744-2756.
32 Campana D, Coustan-Smith E, Janossy G: Double and triple staining methods for studying the proliferative activity of human B and T lymphoid cells. J Immunol Methods 1988;107:79-88.
33 Mosmann T: Rapid colorimetric assay for cellular growth and survival: application to proliferation and cytotoxicity assays. J Immunol Methods 1983;65:55-63.
34 *K*atiyar S, Jiao X, Wagner E, Lisanti MP, Pestell RG: Somatic excision demonstrates that c-Jun induces cellular migration and invasion through induction of stem cell factor. Mol Cell Biol 2007;27:1356-1369.
35 Yang H, Higgins B, Kolinsky K, Packman K, Go Z, Iyer R: RG7204 (PLX4032), a selective BRAFV600E inhibitor, displays potent antitumor activity in preclinical melanoma models. Cancer Res 2010;70:5518-5527.
36 Ichite N, Chougule MB, Jackson T, Fulzele SV, Safe S, Singh M: Enhancement of docetaxel anticancer activity by a novel diindolylmethane compound in human non-small cell lung cancer. Clin Cancer Res 2009;15:543-552.
37 da Rocha Dias S, Salmonson T, van Zwieten-Boot B, Jonsson B, Marchetti S, Schellens JH, Giuliani R, PignattiF: The European Medicines Agency review of vemurafenib (Zelboraf(R)) for the treatment of adult patients with BRAF V600 mutation-positive unresectable or metastatic melanoma: summary of the scientific assessment of the Committee for Medicinal Products for Human Use. Eur J Cancer 2013;49:1654-1661.
38 Chapman PB, Hauschild A, Robert C, Haanen JB, Ascierto P, Larkin J, Dummer R, Garbe C, Testori A, Maio M, Hogg D, Lorigan P, Lebbe C, Jouary T, Schadendorf D, Ribas A, O'Day SJ, Sosman JA, Kirkwood JM, Eggermont AM et al.: Improved survival with vemurafenib in melanoma with BRAF V600E mutation. N Engl J Med 2011;364:2507-2516.
39 Montero-Conde C, Ruiz-Llorente S, Dominguez JM, Knauf JA, Viale A, Sherman EJ: Relief of feedback inhibition of HER3 transcription by RAF and MEK inhibitors attenuates their antitumor effects in BRAF-mutant thyroid carcinomas. Cancer Discov 2013;3:520-533.
40 Prahallad A, Sun C, Huang S, Di Nicolantonio F, Salazar R, Zecchin D, Beijersbergen RL, Bardelli A, Bernards R: Unresponsiveness of colon cancer to BRAF(V600E) inhibition through feedback activation of EGFR. Nature 2012;483:100-103.
41 Jin N, Jiang T, Rosen DM, Nelkin BD, Ball DW: Dual inhibition of mitogen-activated protein kinase kinase and mammalian target of rapamycin in differentiated and anaplastic thyroid cancer. J Clin Endocrinol Metab 2009;94:4107-4112.
42 Jendrzejewski J, Thomas A, Liyanarachchi S, Eiterman A, Tomsic J, He H, Radomska HS, Li W, Nagy R, Sworczak K, de la Chapelle A: PTCSC3 Is Involved in Papillary Thyroid Carcinoma Development by Modulating S100A4 Gene Expression. J Clin Endocrinol Metab 2015;100:E1370-1377.
43 Xing M: Genetic alterations in the phosphatidylinositol-3 kinase/Akt pathway in thyroid cancer. Thyroid 2010;20:697-706.
44 Ringel MD, Hayre N, Saito J, Saunier B, Schuppert F, Burch H, Bernet V, Burman KD, Kohn LD, Saji M: Overexpression and overactivation of Akt in thyroid carcinoma. Cancer Res 2001;61:6105-6111.
45 Vivanco I, Sawyers CL: The phosphatidylinositol 3-Kinase AKT pathway in human cancer. Nat Rev Cancer 2002;2:489-501.
46 Courtney KD, Corcoran RB, Engelman JA: The PI3K pathway as drug target in human cancer. J Clin Oncol 2010;28:1075-1083.
47 McCubrey JA, Steelman LS, Chappell WH, Abrams SL, Wong EW, Chang F, Lehmann B, Terrian DM, Milella M, Tafuri A, Stivala F, Libra M, Basecke J, Evangelisti C, Martelli AM, Franklin RA: Roles of the Raf/MEK/ERK pathway in cell growth, malignant transformation and drug resistance. Biochim Biophys Acta 2007;1773:1263-1284.

48 Porter AP, Papaioannou A, Malliri A: Deregulation of Rho GTPases in cancer. Small GTPases 2016;7:123-138.
49 Chen M, Bresnick AR, O'Connor KL: Coupling S100A4 to rhotekin alters Rho signaling output in breast cancer cells. Oncogene 2013;32:3754-3764
50 *Solit DB, Rosen N:* Resistance to BRAF inhibition in melanomas. *N Engl J Med 2011;364:772-774.*
51 Straussman R, Morikawa T, Shee K, Barzily-Rokni M, Qian ZR, Du J, Davis A, Mongare MM, Gould J, Frederick DT, Cooper ZA, Chapman PB, Solit DB, Ribas A, Lo RS, Flaherty KT, Ogino S, Wargo JA, Golub TR: Tumour micro-environment elicits innate resistance to RAF inhibitors through HGF secretion. Nature 2012;487:500-504.
52 Byeon HK, Na HJ, Yang YJ, Ko S, Yoon SO, Ku M, Yang J, Kim JW, Ban MJ, Kim JH[7], Kim DH, Kim JM, Choi EC, Kim CH, Yoon JH, Koh YW: Acquired resistance to BRAF inhibition induces epithelial-to-mesenchymaltransition in BRAF (V600E) mutant thyroid cancer by c-Met-mediated AKT activation. Oncotarget 2017;8:596-609.
53 Bollag G, Hirth P, Tsai J, Zhang J, Ibrahim PN, Cho H, Spevak W, Zhang C, Zhang Y, Habets G, Burton EA, Wong B, Tsang G, West BL, Powell B, Shellooe R, Marimuthu A, Nguyen H, Zhang KY, Artis DR et al.: Clinical efficacy of a RAF inhibitor needs broad target blockade in BRAF-mutant melanoma. Nature 2010;467:596-599.
54 Chan CM, Jing X, Pike LA, Zhou Q, Lim DJ, Sams SB, Lund GS, Sharma V, Haugen BR, Schweppe RE: Targeted inhibition of Src kinase with dasatinib blocks thyroid cancer growth and metastasis. Clin Cancer Res 2012;18:3580-3591.
55 Nucera C, Nehs MA, Mekel M, Zhang X, Hodin R, Lawler J, Nose V, Parangi S: A novel orthotopic mouse model of human anaplastic thyroid carcinoma. Thyroid 2009;19:1077-1084.
56 Stein U, Arlt F, Walther W, Smith J, Waldman T, Harris ED, Mertins SD, Heizmann CW, Allard D, Birchmeier W, Schlag PM, Shoemaker RH: The metastasis-associated gene S100A4 is a novel target of beta-catenin/T-cell factor signaling in colon cancer. Gastroenterology 2006;131:1486-1500.
57 Killion JJ, Radinsky R, Fidler IJ: Orthotopic models are necessary to predict therapy of transplantable tumors in mice. Cancer Metastasis Rev 1998;17:279-284.
58 Sharkey FE, Fogh J: Metastasis of human tumors in athymic nude mice. Int J Cancer 1979;24:733-738.